Electronic structure of $(Ce_{1-x}Nd_x)_3Al$ probed by resonant x-ray emission spectroscopy

Hitoshi Yamaoka,[1] Ignace Jarrige,[2] Ryoichi Yamagata,[3] Katsuhiko Nishimura,[3] Nozomu Hiraoka,[4] Hirofumi Ishii,[4] and Ku-Ding Tsuei[4]

[1]*Harima Institute, The Institute of Physical and Chemical Research (RIKEN), Sayo, Hyogo 679-5148, Japan*

[2]*Synchrotron Radiation Research Unit, Japan Atomic Energy Agency, 1-1-1 Kouto, Sayo, Hyogo 679-5148, Japan*

[3]*Graduate School of Science and Engineering, University of Toyama, Toyama 930-8555, Japan*

[4]*National Synchrotron Radiation Research Center, Hsinchu 30076, Taiwan*

(Received 26 November 2009; revised manuscript received 27 January 2010; published 30 March 2010)

Bulk-sensitive measurements of the electronic structure of Ce in the $(Ce_{1-x}Nd_x)_3Al$ system have been performed as a function of temperature and x using x-ray absorption spectroscopy in the partial fluorescence yield mode and resonant x-ray emission spectroscopy (RXES) at the Ce L_3 edge. In the Ce-rich samples, the RXES spectra indicate a mixed-valence state consisting mainly of f^1 with a small fraction of f^0 and f^2. The f^1/f^2 intensity ratio is found to undergo a first-order transition at low temperature, coinciding with the $\alpha \rightarrow \gamma$ structural transition. Following the disappearance of the Kondo effect at $x>0.2$, the f^1/f^2 intensity ratio is found to significantly increase with x, signifying a weakening of the mixed-valence character. The fact that the volume remains nearly constant upon Nd doping points to an electronic origin of the x dependence of the Ce f^1/f^2 intensity ratio.

DOI: 10.1103/PhysRevB.81.115137 PACS number(s): 72.15.Qm, 75.30.Mb, 78.70.En, 78.70.Dm

I. INTRODUCTION

Ce-based intermetallic compounds have generated considerable interest owing to their exotic, heavy fermionlike physical properties such as a large electronic specific coefficient, valence fluctuation, Kondo effect, and magnetic ordering.[1,2] These unusual properties are normally attributed to the peculiar behavior of the atomiclike $4f$ states and their hybridization with the band of conduction electrons, competing with the Ruderman-Kittel-Kasuya-Yoshida (RKKY) interaction.

Among the (Ce,Al)-based compounds, the R_3Al (R: rare earth) system has attracted much attention. R_3Al has a Ni_3Al-type hexagonal crystal structure with the space group $P6/mmc$ at room temperature. Ce_3Al is an archetypal heavy fermion system with a large electronic specific coefficient of the order of 100 $mJ/K^2/Ce\text{-}mol$.[3–17] Upon cooling, a structural transition from α (hexagonal) to γ (monoclinic) occurs at $T_S=110$ K accompanied by a volume contraction of about 9%, and antiferromagnetic order sets in at $T_N=2.2$ K.[9,11] At $T<1$ K the specific heat shows Fermi-liquid behavior. The temperature dependence of the resistivity shows a minimum around 20 K, suggesting single impurity Kondo regime.[16] Using Ce-3d photoelectron spectroscopy (PES), it was shown that at $T \leq T_S$ the Ce^{4+} ($4f^0$) weight increases, pointing to increased valence fluctuation and Kondo effect.[7] At $T>500$ K Ce_3Al has a β phase with cubic structure. Zeng *et al.*[18] succeeded in synthesizing the β phase fcc Ce_3Al at room temperature under high pressure. Their study showed that the electronic transition accompanying the structural transition is reversible after decompression to ambient pressure, whereas the structural transition is not.

On the other hand, the ferromagnet Nd_3Al has been recently successfully synthesized.[19] Nd_3Al shows paramagnetic to ferromagnetic transition at $T_C=74$ K. Below T_C the resistivity decreases monotonically and below 10 K it is not proportional to T^2, respectively, indicating the absence of single impurity Kondo region and of a Fermi-liquid ground state. Therefore, the substitution of Nd to Ce sites in Ce_3Al offers the interesting opportunity to span the competing interactions between magnetic orderings and the Kondo effect. Recently Li *et al.* reported the lattice parameter, electrical resistivity, magnetization, and specific heat of $(Ce_{1-x}Nd_x)_3Al$.[20] Both T_N and T_S rapidly decrease upon Nd substitution until vanishing at $x=0.1$ and 0.4 respectively, as ferromagnetism sets in at $x \geq 0.2$, T_C increasing linearly with x. The low-temperature resistivity shows $\log-T$ dependence for $x \leq 0.3$, implying occurrence of single impurity Kondo effect. At $x \geq 0.35$, the Kondo effect disappears, coinciding with the α to γ phase transition upon x increase at low temperature and its associated volume increase. In order to elucidate these rich physical properties, a thorough investigation of the electronic structure is necessary. It is what we aim to provide with the present study.

In this paper, we report an x-ray spectroscopic study of the electronic structure of $(Ce_{1-x}Nd_x)_3Al$ as a function of both x and temperature. We employ two complementary hard x-ray spectroscopic probes at the Ce L_3 edge, partial fluorescence yield x-ray absorption spectroscopy (PFY-XAS) and resonant x-ray emission spectroscopy (RXES).[21–26] For the Ce-rich systems ($x \leq 0.2$), we observe in the temperature dependence of the f^1/f^2 ratio a first-order transition coinciding with the $\alpha \rightarrow \gamma$ transition. After the Kondo effect vanishes at $x>0.2$, the f^1/f^2 intensity ratio is found to monotonically increase with x, pointing to a decrease in the Ce mixed-valence character upon Nd doping.

II. EXPERIMENTS

$(Ce_{1-x}Nd_x)_3Al$ polycrystalline samples were prepared for $x=0$, 0.05, 0.15, 0.25, 0.35, 0.5, and 1.0 by an arc melting method under argon atmosphere. Detailed information of the structure, magnetic ordering and other transport properties can be found in Ref. 20. The temperature dependence of the

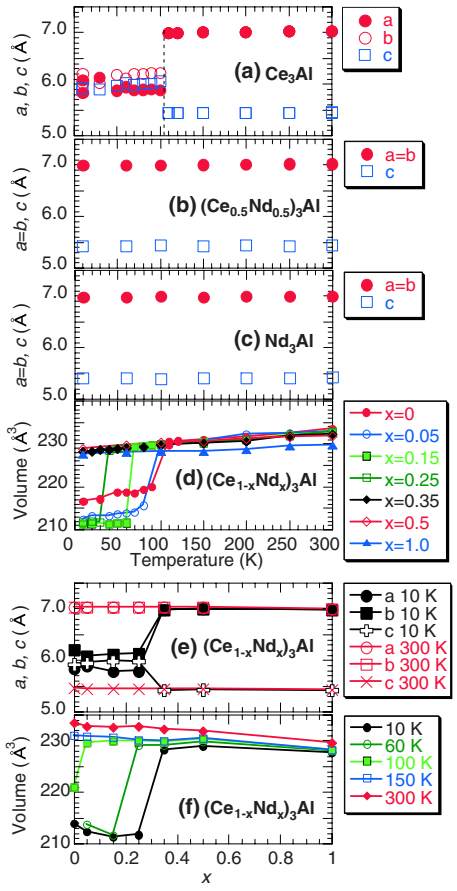

FIG. 1. (Color online) (a)–(c) Change in lattice parameters as a function of temperature at $x=0$, 0.5, and 1.0. (d) Change in volume as a function of temperature for given x. (e) x dependence of lattice parameters at 10 and 300 K. (f) Change in volume as a function of x for given temperatures.

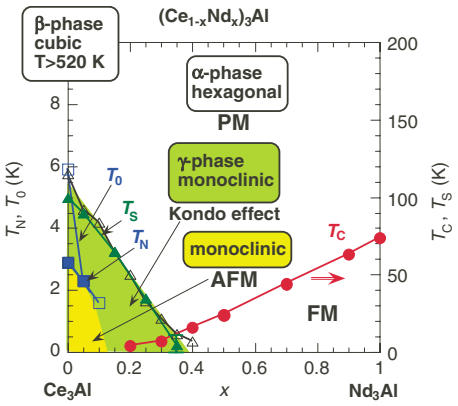

FIG. 2. (Color online) Phase diagram of $(Ce_{1-x}Nd_x)_3Al$. x dependences of characteristic temperature (Ref. 20) (T_0, open square), Néel temperature (T_N, closed square), structural transition temperature (T_S, closed triangle: from x-ray diffraction, open triangle: from resistivity measurement), and magnetic transition temperature from paramagnet to ferromagnet (T_C, closed circle) are shown, respectively. The data are taken from Ref. 20 except T_S obtained by the x-ray diffraction (this work).

crystal structure is measured by x-ray diffraction (XRD), using a Rigaku RINT2000 diffractometer. PFY-XAS and RXES measurements were performed at the Taiwan beamline BL12XU at SPring-8.[27] The undulator beam was monochromatized by a pair of Si(111) crystals and focused to a spot of about 120 (horizontal) $\times 80$ (vertical) μm^2 at the sample position using a toroidal mirror. The samples were at 45° to the direction of the incident beam and the radiation scattered from the sample at 90° from the direction of the incident beam was analyzed. Incident photon energies are calibrated by using metal K-absorption edges of V and Cr. A Johann-type spectrometer equipped with a spherically bent (~1 m) Si(400) crystal was used to analyze the Ce $L\alpha_1$ ($3d_{5/2} \rightarrow 2p_{3/2}$) emission line. The overall energy resolution was about 1.5 eV. A closed-circuit He cryostat was used for the low-temperature measurements.

III. RESULTS AND DISCUSSION

A. Phase diagram

We measure both temperature (T) and x dependences of the lattice parameters. Ce_3Al shows a structural transition at $T_S=110$ K as shown in Fig. 1(a) in agreement with a previous measurement.[6] In the low-temperature phase, a and b contract and c expands, yielding a monoclinic structure where all three axes have close values. This is the so-called $\alpha \rightarrow \gamma$ structural transition, observed to take place at $x \leq 0.35$ as seen in Fig. 1(d). The volume contraction at T_S is found to be within 6%–9%. At $x \geq 0.35$, only a slight, monotonic volume contraction upon cooling is observed. The measured values of T_S are summarized in Fig. 2 as a function of x and T, along with T_C, T_N, and T_0, which is related to the Kondo temperature. According to the Bethe-Ansatz solution of the Coqblin-Schrieffer model, the physical properties of a Kondo lattice are well scaled by a single energy parameter (T_0).[28,29] We used the T_0 estimated through the fitting the Rajan's curve to the experimental result of the magnetic susceptibility with taking into account the crystal-field effect.[20]

The values of T_S measured by XRD agree well with the resistivity measurement of Ref. 20. At low temperature there is a crossover of the structural and magnetic transitions between $x=0.2$ and 0.4. Ce-rich samples, in the limited region of $x \leq 0.1$, display an antiferromagnetic transition around 2 K. Resistivity measurements indicate a Kondo minimum in the same region,[20] pointing to an increased $c-f$ hybridization between the conduction band and the f states. A small proportion of substituted Nd atoms strongly dilute the Kondo effect. Chen *et al.* observed the coexistence of magnetic ordering and Kondo behavior in the antiferromagnetic phase of (Ce,Al)-based compounds.[15,17] Our results here suggest a similar phenomenon for the Ce-rich $(Ce_{1-x}Nd_x)_3Al$. In $(Ce_{1-x}La_x)_3Al$, the enhancement of T_0 accompanying the volume contraction with decreasing La concentration x was reported to coincide with the decrease of T_N.[15] This is consistent with the competition between Kondo effect and the RKKY interaction. This is, however, in contrast with Nd substitution to the Ce site which causes both T_0 and T_N to concomitantly decrease due to the increase of the ferromagnetic local-moment character.

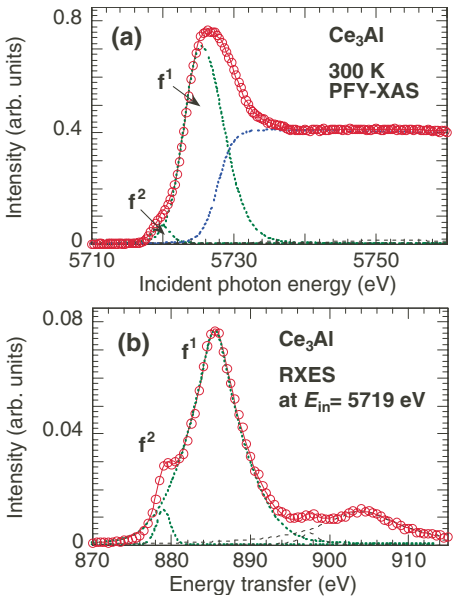

FIG. 3. (Color online) Examples of the curve fit for (a) PFY-XAS and (b) RXES at E_{in}=5719 eV of the x=0 sample at 300 K, respectively. Open circles and solid line correspond to the experimental data and total intensity of fit curves, respectively.

B. x dependence of the electronic structure

The fits of the PFY-XAS and RXES at E_{in}=5719 eV spectra are shown for Ce_3Al at 300 K as examples in Figs. 3(a) and 3(b), respectively, where E_{in} is incident photon energy.[21–26] After subtraction of an arctangent-like (asymmetrical double sigmoid) function corresponding to the continuum excitations, two Voigt functions are used to fit the f^1 (Ce^{3+}) component centered at 5726 eV and the f^2 (Ce^{2+}) contribution around 5718 eV. For the fit of the RXES spectra, we use a pseudo-Voigt function for f^1 and Voigt functions for the other components. As will be shown in the analysis of the RXES spectra in Sec. III D, a small fraction of f^0 (Ce^{4+}) is also present, hidden by the high-energy tail of the f^1 peak in the PFY-XAS spectrum. The x dependence of the Ce L_3 PFY-XAS spectra measured at 300 and 22 K is shown in Figs. 4(a) and 4(d). We note that the intensity of the spectra is normalized by the area of the $L\alpha_1$ fluorescence spectrum collected for all samples at an incident photon energy of E_{in}=5760 eV. Figures 4(b) and 4(e) show the difference between the PFY-XAS spectra for the different values of x measured and the spectrum for Ce_3Al. The x dependence of the intensity ratio of f^1 to f^2, derived from the fits of the spectra in Figs. 4(a) and 4(d), is shown in Figs. 4(c) and 4(f). The ratio is found to be nearly constant over x=0–0.2, and grows monotonically with x at $x>0.2$. We note that the range of the vertical axis of Figs. 4(c) and 4(f) is too large to allow for observing the small variations in the f^1/f^2 intensity ratio between 300 and 22 K at $x<0.35$ (namely, across the $\alpha \rightarrow \gamma$ transition). These variations are investigated in detail in the next section. The increase in f^1 at the detriment of f^2 with increasing x suggests a decrease in the interaction between the f and the itinerant d states, in accord with the suppression of the Kondo effect. It is consistent with the resistivity decrease upon x increase[20] which indicates an increase of the number of conduction-band electrons. In turn, this change in the density of conduction states might also cause a shift of the Fermi level, accounting for the fact that the local-moment character starts to dominate. At $x \leq 0.25$

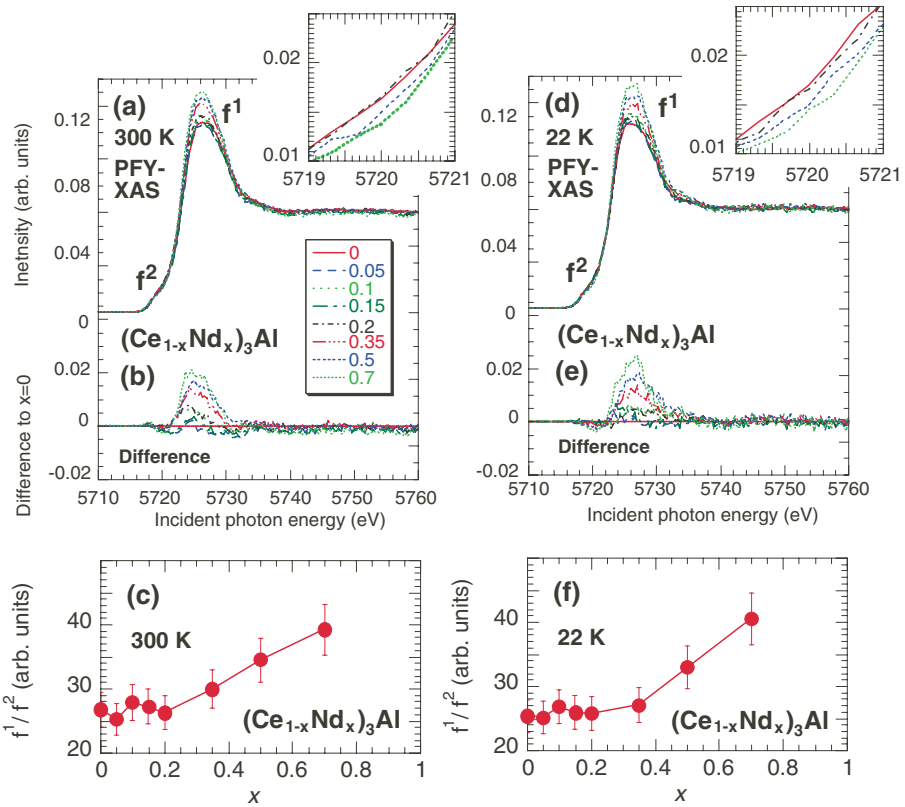

FIG. 4. (Color online) x dependence the Ce L_3 PFY-XAS spectra measured at (a) 300 and (d) 22 K with enlarged parts of figures at right-upper sides. In (b) and (e) the differences of the PFY-XAS intensity to the intensity at x=0 are shown. In (c) and (f) the intensity ratio of f^1 to f^2, obtained from the curve fit for the data in (a) and (d), are also shown.

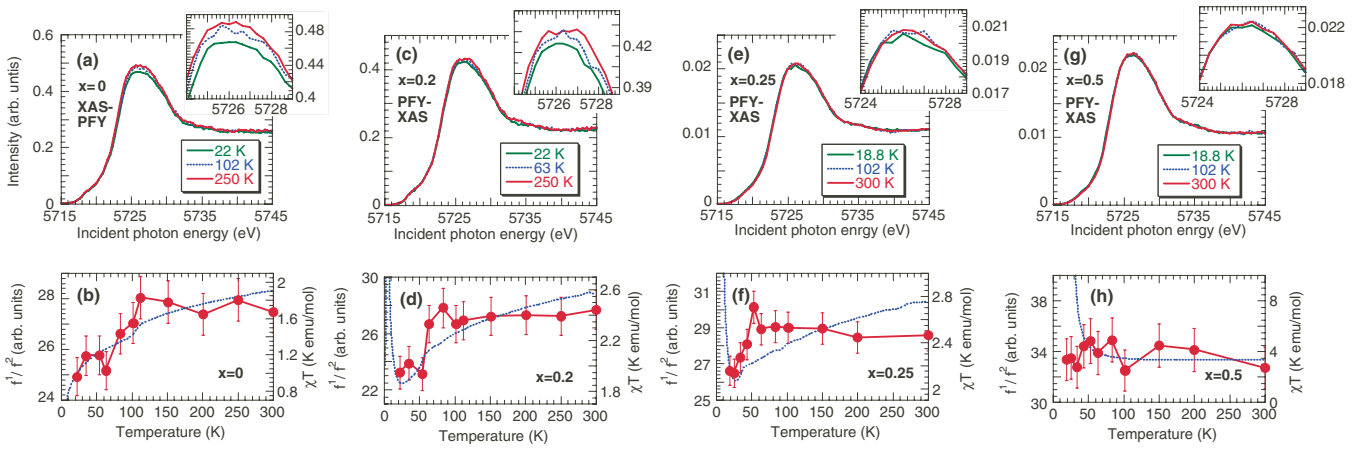

FIG. 5. (Color online) Temperature dependence of the Ce L_3 PFY-XAS spectra measured for (a) $x=0$ (Ce_3Al), (c) $x=0.2$, (e) $x=0.25$, and (g) $x=0.5$ with enlarged parts of figures at right-upper sides. Change in the intensity ratio of f^1 to f^2 as a function of temperature is shown for (b) $x=0$ (d) $x=0.2$, (f) $x=0.25$, and (h) $x=0.5$. Dashed lines in (b), (d), (f), and (h) correspond to the χT curves, where χ and T are magnetic susceptibility and temperature, respectively.

the Kondo effect competes with the moment localization induced by the Nd substitution. Around $x \geq 0.3$ the Kondo effect on the Ce sites disappears and the Ce f^1 intensity monotonically increases, while the magnetic character of both Ce and Nd governs.[20] A similar electron-doping effect was also observed in $Yb_{1-x}Lu_xAl_3$ (Ref. 33) and $Ce(Pd_{1-x}Cu_x)_3$,[34] with a shift of the Fermi level concomitant to a change in the Kondo temperature.

The increase in the Ce f^1/f^2 intensity ratio with x is likely to have an electronic origin, since the volume of the unit cell is almost independent of x. Trivalent in $EuPd_3$, Eu in $Ce_{0.5}Eu_{0.5}Pd_3$ was recently reported to be in a mixed-valent state, seemingly induced by a charge transfer between the $4f$ states of Ce and Eu.[35] This case stresses the importance of the $4f-4f$ interactions and their possible consequence on the f occupancy when two different rare-earth ions are present in the same unit cell. Similarly in $(Ce_{1-x}Nd_x)_3Al$, a charge transfer from Ce $4f$ to Nd $4f$, enhanced as x increases, could account for the increase of the Ce f^1/f^2 intensity ratio. The knowledge of the Nd electronic structure would be necessary to ascertain this hypothesis.

C. Temperature dependence of the electronic structure

Figures 5(a), 5(c), 5(e), and 5(g) show the temperature dependence of the PFY-XAS spectra measured at $x=0$, 0.2, 0.25, and 0.5, respectively. The corresponding temperature dependence of the f^1 to f^2 intensity ratio is displayed in Figs. 5(b), 5(d), 5(f), and 5(h), respectively. In the $x=0$, 0.2, and 0.25 samples, the f^1/f^2 intensity ratio decreases abruptly upon cooling at the $\alpha \rightarrow \gamma$ structural transition ($\sim$100, 70, and 50 K respectively), as a direct consequence of the volume contraction associated with the transition. On the other hand, at $x=0.5$ the f^1/f^2 intensity ratio is unchanged throughout the 20–300 K range within the error bars, in accordance with the absence of $\alpha \rightarrow \gamma$ structural transition.

In Ce metal McMahan *et al.*[30] showed by LDA+DMFT calculations that at the $\gamma \rightarrow \alpha$ transition, while the volume decreases in $\Delta V/V \sim 14\%$, the fraction of f^1 decreases and those of f^0 and f^2 increase. Experimentally, the relative decrease in the f^1 component with respect to f^2 was evidenced by Rueff *et al.*[31] and Dallera *et al.*[32] using the RXES. Although $(Ce_{1-x}Nd_x)_3Al$ undergoes a reversed transition from α to γ with decreasing temperature, the relation between the relative change in the f^1 intensity and the volume is basically the same as Ce metal and other Ce alloys: the decrease in the volume causes the relative decrease of the f^1 intensity, as seen in the lower panels of Fig. 5.

In a former Ce-$3d$ PES study on Ce_3Al, both f^0 and f^2 intensities were found to increase abruptly by 10% at the transition around 120 K when the spectrum intensity is normalized to the f^1 peak,[7] in good agreement with our study. Sakurai *et al.* estimated the decrease of magnetic moment to about 20% at low temperature, hinting at an increase in the Kondo effect across the $\alpha \rightarrow \gamma$ transition.[6]

In lower panels in Fig. 5 we also show the temperature dependence of χT, where χ is the magnetic susceptibility.[20] We find a jump in the χT curves at 110 K for $x=0$, 50–60 K for $x=0.2$, and 30 K for $x=0.25$ which systematically coincides with the $\alpha \rightarrow \gamma$ transition. The temperature dependence of the f^1 intensity seemingly follows that of χT at $x=0$, 0.2, and 0.25. In Yb compounds we observed close similarities between the temperature dependence of the rare-earth valence and of χT.[25,26] This is well understood because the decrease in χT with temperature originates from the concomitant decrease in the magnetic Yb^{3+} component, Yb^{2+} being nonmagnetic. In the Ce system both $4f^2$ and $4f^1$ configurations are magnetic and $4f^0$ is nonmagnetic. Both f^0 and f^2 components increase below 120 K based on PES,[7] and f^1 decreases according to both PES and our RXES study. It seems here that the temperature-induced f^1 decrease can explain the temperature dependence of χT in a similar fashion as for Yb compounds for the $x=0$, 0.2, and 0.25 samples.

D. Resonant Raman spectra

The E_{in} dependence of the Ce $2p_{3/2}$-$3d_{5/2}$ RXES spectrum across the L_3 edge is shown in Fig. 6 for Ce_3Al ($x=0$) at both

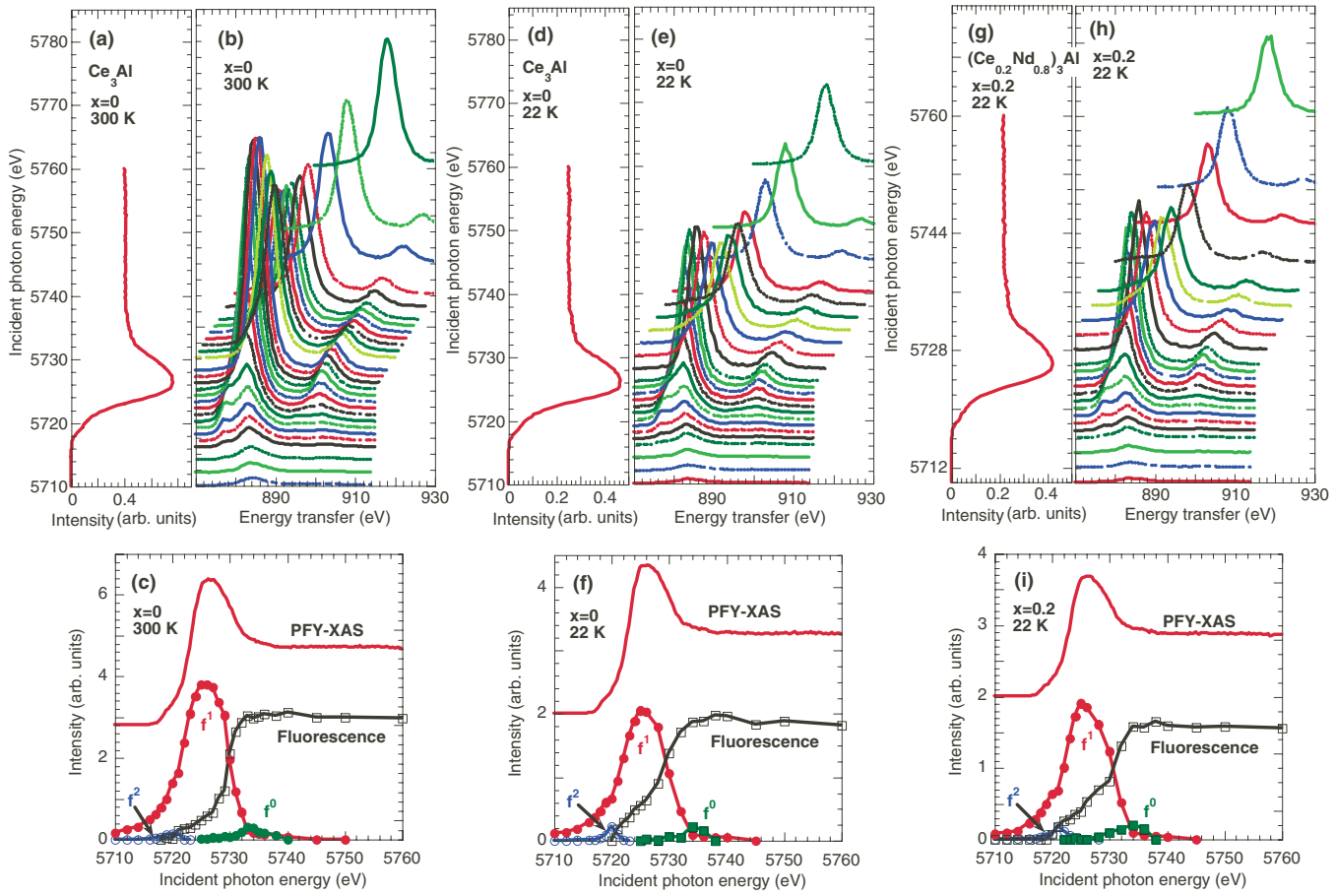

FIG. 6. (Color online) Ce $2p_{3/2}$-$3d_{5/2}$ RXES spectra as a function of incident photon energies of E_{in} across the L_3 edge for (a)–(c) Ce_3Al ($x=0$) at 300 K, (d)–(f) Ce_3Al at 22 K, and (g)–(i) $x=0.2$ sample at 22 K. The vertical position of the each RXES spectra in the panel (b), (e), and (h) corresponds to the E_{in} of PFY-XAS spectrum they were measured at in the panel (a), (d), and (g), respectively. The E_{in} dependence of the respective components fitted to the RXES spectra (Raman f^0: closed square, f^1: closed circle, f^2: open circle, and fluorescence: open square) is shown in (c), (f), and (i) with the PFY-XAS spectra.

300 and 22 K and for the $x=0.2$ sample at 22 K. For E_{in} up to the maximum of the white line, the spectra are found to be in the so-called Raman regime with a constant energy transfer, which is defined as the difference between the incident and emitted photon energies. The best fit was obtained with three Raman components, respectively, corresponding to f^0, f^1, and f^2. The E_{in} dependence of those components and of the $L\alpha_1$ fluorescence is shown in Figs. 6(c), 6(f), and 6(i) along with the PFY-XAS spectrum. We estimated the mean valence using the formula $v=3+\{I(f^0)-I(f^2)\}/\{I(f^1)+I(f^2)+I(f^0)\}$, where $I(f^n)$ is the intensity of the f^n component. We obtain 3.02 ± 0.05 for Ce_3Al at 300 K, 3.02 ± 0.05 for Ce_3Al at 22 K, and 3.05 ± 0.05 for $x=0.2$ at 22 K. The corresponding intensity ratios in percentage are f^0: f^1: $f^2=3.8$: 94.5: 1.7 for $x=0$ at 300 K, 4.3: 93.4: 2.3 for $x=0$ at 22 K, and 7.4: 89.8: 2.8 for $x=0.2$ at 22 K. The Ce valence for $x=0$, 0.2 is therefore nearly 3+, with small finite components of f^2 and f^0, indicating a slightly intermediate-valent state. The valence is found to be only weakly dependent on temperature and x for the considered systems. Experimentally derived values of the magnetic moment for these systems were best reproduced by calculations assuming trivalent Ce and Nd ions,[20] in good agreement with our results.

IV. CONCLUSION

We have studied both composition and temperature dependences of the electronic structure of $(Ce_{1-x}Nd_x)_3Al$ using bulk-sensitive x-ray spectroscopies, PFY-XAS and RXES. The results show a small valence fluctuation in the Ce-rich systems, consisting mainly of f^1 with a small fraction of f^0 and f^2. At $x\leq0.25$ the change in the f^1 to f^2 intensity ratio as a function of temperature follows the change in the volume accompanying the $\alpha\rightarrow\gamma$ structural phase transition. A small substitution of Nd at the Ce sites strongly dilutes the Kondo effect and the f^1 to f^2 intensity ratio becomes invariant over temperature with the onset of the AF order. The fact that the volume remains nearly constant upon Nd doping points to a possibility of an electronic origin of the change in the f^1/f^2 intensity ratio with x such as Nd $4f$-Ce $4f$ charge transfer.

ACKNOWLEDGMENTS

The experiments were performed at Taiwan beamline BL12XU (SPring-8 under proposal No. 2008B4255 and NSRRC project No. 2008-3-007-1) of SPring-8, Japan Synchrotron Radiation Research Institute (JASRI).

[1] E. Bauer, Adv. Phys. **40**, 417 (1991).
[2] G. R. Stewart, Rev. Mod. Phys. **73**, 797 (2001).
[3] J. D. Thompson, Z. Fisk, Y. Y. Chen, and J. M. Lawrence, J. Less Common Met. **127**, 385 (1987).
[4] M. Sera, T. Satoh, and T. Kasuya, J. Magn. Magn. Mater. **63–64**, 82 (1987).
[5] J. Sakurai, T. Matsuura, and Y. Komura, J. Phys. Colloq. **49/C8**, 783 (1988).
[6] J. Sakurai, Y. Murashita, Y. Aoki, T. Fujita, T. Takabatake, and H. Fujii, J. Phys. Soc. Jpn. **58**, 4078 (1989).
[7] K. Okuda, S. Noguchi, Y. Takigawa, Y. Murashita, J. Sakurai, and H. Fujii, J. Phys. Soc. Jpn. **58**, 2630 (1989).
[8] C. S. Garde, J. Ray, and G. Chandra, J. Phys.: Condens. Matter **1**, 2737 (1989).
[9] Y. Y. Chen, J. M. Lawrence, J. D. Thompson, and J. O. Willis, Phys. Rev. B **40**, 10766 (1989).
[10] A. C. Lawson, J. M. Lawrence, J. D. Thompson, and A. Williams, Physica B **163**, 587 (1990).
[11] T. Suzuki, Y. Aoki, S. Nishigori, T. Fujita, Y. Murashita, and J. Sakurai, J. Magn. Magn. Mater. **90-91**, 482 (1990).
[12] S. Y. Wu, W. T. Hsieh, W.-H. Li, and K. C. Lee, Chin. J. Phys. **31**, 663 (1993).
[13] T. Kagayama and G. Oomi, J. Phys. Soc. Jpn. **65**, Suppl. B, 42 (1996).
[14] L. S. Azechi, A. N. Medina, and F. G. Gandra, J. Appl. Phys. **81**, 4179 (1997).
[15] Y. Y. Chen, Y. D. Yao, B. C. Hu, C. H. Jang, J. M. Lawrence, H. Huang, and W. H. Li, Phys. Rev. B **55**, 5937 (1997).
[16] A. N. Medina, M. A. Hayashi, L. P. Cardoso, S. Gama, and F. G. Gandra, Phys. Rev. B **57**, 5900 (1998).
[17] Y. Y. Chen, Y. D. Yao, C. R. Wang, W. H. Li, C. L. Chang, T. K. Lee, T. M. Hong, J. C. Ho, and S. F. Pan, Phys. Rev. Lett. **84**, 4990 (2000).
[18] Q.-S. Zeng, Y. Ding, W. L. Mao, W. Luo, A. Blomqvist, R. Ahuja, W. Yang, J. Shu, S. V. Sinogeikin, Y. Meng, D. L. Brewe, J.-Z. Jiang, and H.-k. Mao, Proc. Natl. Acad. Sci. U.S.A. **106**, 2515 (2009).
[19] T. Fukuhara, R. Yamagata, L. Li, K. Nishimura, and K. Maezawa, J. Phys. Soc. Jpn. **78**, 034723 (2009).
[20] L. Li, R. Yamagata, K. Nishimura, and H. Yamaoka, Phys. Rev. B **80**, 134429 (2009).
[21] I. Jarrige, H. Ishii, Y. Q. Cai, J.-P. Rueff, C. Bonnelle, T. Matsumura, and S. R. Shieh, Phys. Rev. B **72**, 075122 (2005).
[22] H. Yamaoka, M. Taguchi, A. M. Vlaicu, H. Oohashi, Y. Yokoi, D. Horiguchi, T. Tochio, Y. Ito, K. Kawatsura, K. Yamamoto, A. Chainani, S. Shin, M. Shiga, and H. Wada, J. Phys. Soc. Jpn. **75**, 034702 (2006).
[23] H. Yamaoka, N. Tsujii, K. Yamamoto, H. Oohashi, A. M. Vlaicu, K. Kunitani, K. Uotani, D. Horiguchi, T. Tochio, Y. Ito, and S. Shin, Phys. Rev. B **76**, 075130 (2007).
[24] H. Yamaoka, H. Oohashi, I. Jarrige, T. Terashima, Y. Zou, H. Mizota, S. Sakakura, T. Tochio, Y. Ito, E. Ya. Sherman, and A. Kotani, Phys. Rev. B **77**, 045135 (2008).
[25] H. Yamaoka, N. Tsujii, K. Yamamoto, A. M. Vlaicu, H. Oohashi, H. Yoshikawa, T. Tochio, Y. Ito, A. Chainani, and S. Shin, Phys. Rev. B **78**, 045127 (2008).
[26] H. Yamaoka, I. Jarrige, N. Tsujii, N. Hiraoka, H. Ishii, and K.-D. Tsuei, Phys. Rev. B **80**, 035120 (2009).
[27] Y. Q. Cai, P. Chow, C. C. Chen, H. Ishii, K. L. Tsang, C. C. Kao, K. S. Liang, and C. T. Chen, AIP Conf. Proc. **705**, 340 (2004).
[28] B. Coqblin and J. R. Schrieffer, Phys. Rev. **185**, 847 (1969).
[29] V. T. Rajan, Phys. Rev. Lett. **51**, 308 (1983).
[30] A. K. McMahan, K. Held, and R. T. Scalettar, Phys. Rev. B **67**, 075108 (2003).
[31] J.-P. Rueff, C. F. Hague, J.-M. Mariot, L. Journel, R. Delaunay, J.-P. Kappler, G. Schmerber, A. Derory, N. Jaouen, and G. Krill, Phys. Rev. Lett. **93**, 067402 (2004).
[32] C. Dallera, M. Grioni, A. Palenzona, M. Taguchi, E. Annese, G. Ghiringhelli, A. Tagliaferri, N. B. Brookes, Th. Neisius, and L. Braicovich, Phys. Rev. B **70**, 085112 (2004).
[33] J. Yamaguchi, A. Sekiyama, S. Imada, A. Yamasaki, M. Tsunekawa, T. Muro, T. Ebihara, Y. Ōnuki, and S. Suga, New J. Phys. **9**, 317 (2007).
[34] S. Kasai, S. Imada, A. Yamasaki, A. Sekiyama, F. Iga, M. Kasaya, and S. Suga, J. Electron Spectrosc. Relat. Phenom. **156-158**, 441 (2007).
[35] A. Pandey, C. Mazumdar, R. Ranganathan, V. R. Reddy, and A. Gupta, Appl. Phys. Lett. **94**, 182503 (2009).